Current Biology, Volume *26*

Supplemental Information

The Demographic Development of the First Farmers in Anatolia

Gülşah Merve Kılınç, Ayça Omrak, Füsun Özer, Torsten Günther, Ali Metin Büyükkarakaya, Erhan Bıçakçı, Douglas Baird, Handan Melike Dönertaş, Ayshin Ghalichi, Reyhan Yaka, Dilek Koptekin, Sinan Can Açan, Poorya Parvizi, Maja Krzewińska, Evangelia A. Daskalaki, Eren Yüncü, Nihan Dilşad Dağtaş, Andrew Fairbairn, Jessica Pearson, Gökhan Mustafaoğlu, Yılmaz Selim Erdal, Yasin Gökhan Çakan, İnci Togan, Mehmet Somel, Jan Storå, Mattias Jakobsson, and Anders Götherström

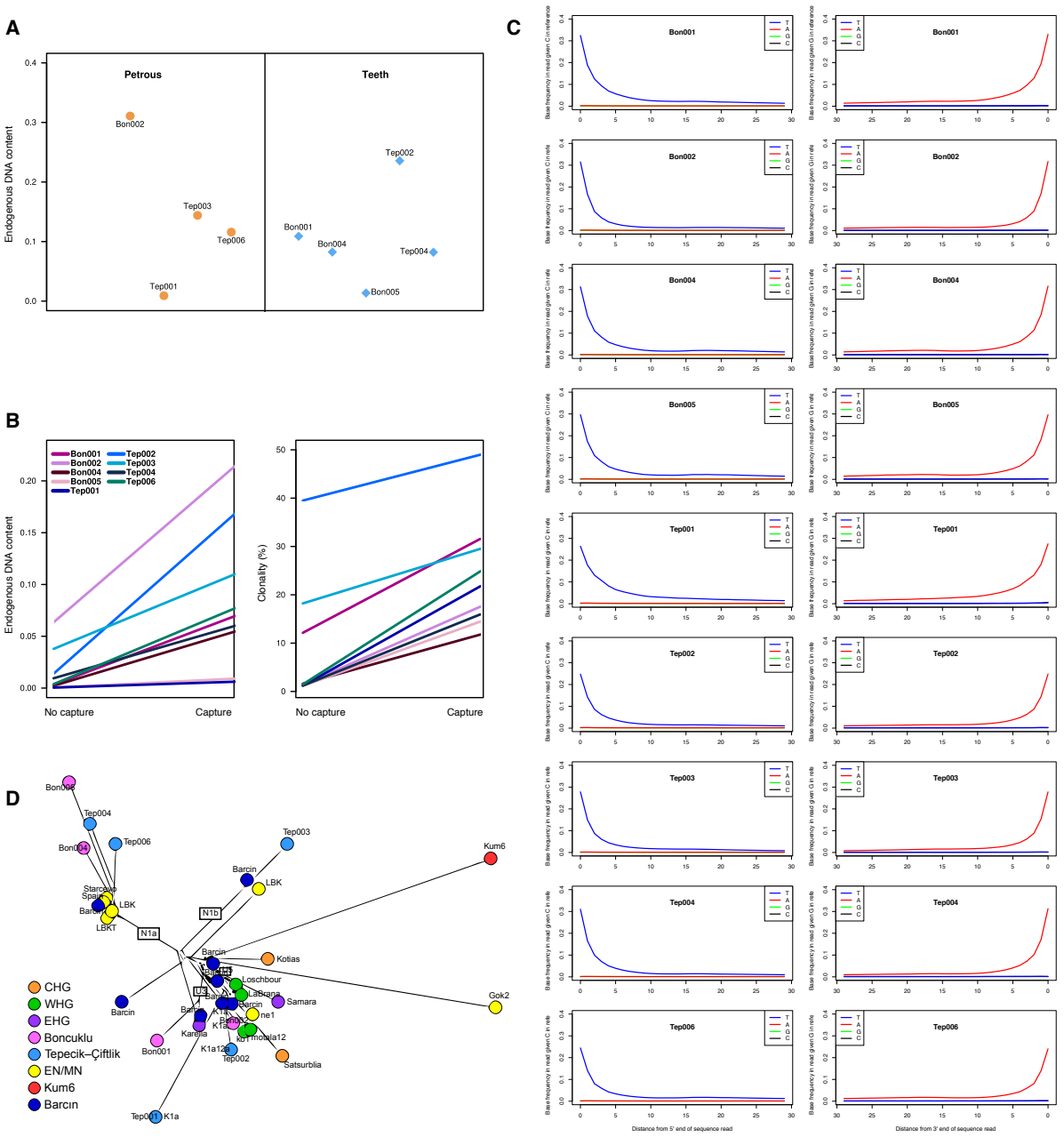

Figure S1. A) Mean endogenous aDNA content in individuals obtained from teeth and petrous bone. B) Mean endogenous aDNA content and clonality of the whole genome capture vs non-capture libraries. C) Nucleotide misincorporation patterns in Boncuklu and Tepecik-Çiftlik individuals. D) Mitochondrial DNA haplogroup network. CHG: Caucasus hunter-gatherer, WHG: West European hunter-gatherer, EHG: East European hunter-gatherer, EN: Early European Neolithic, MN: Middle European Neolithic (Related to Figure 1)

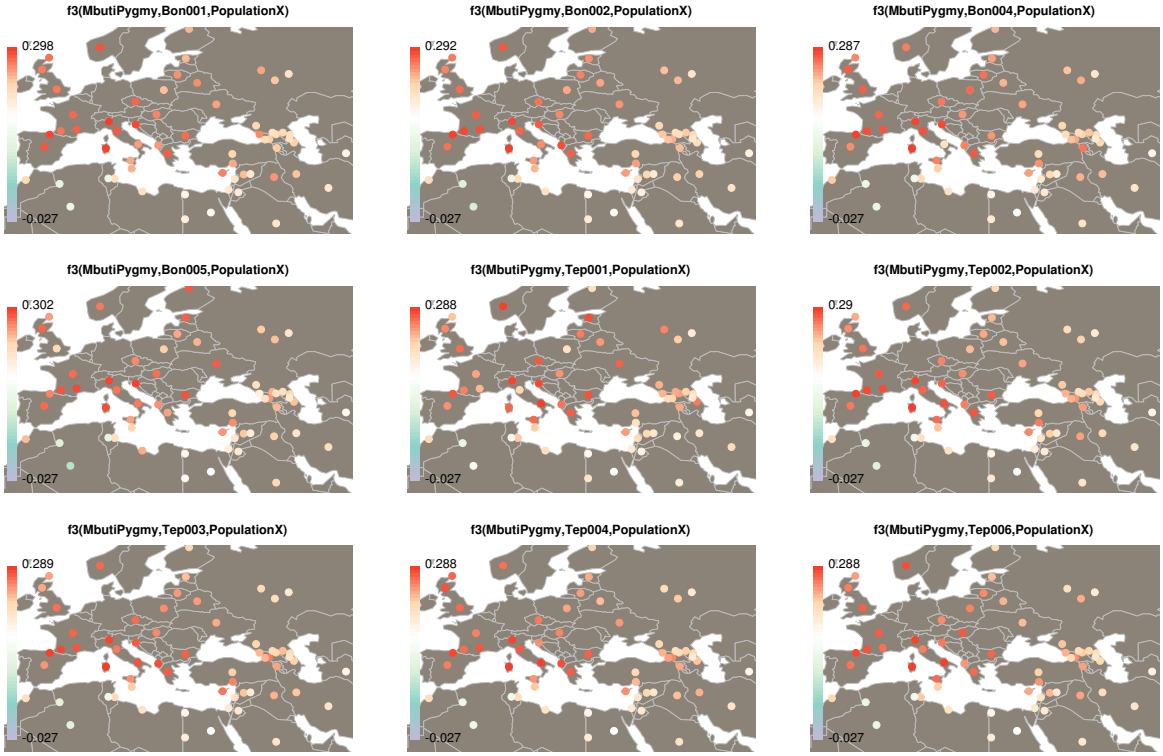

Figure S2. Shared genetic drift between ancient individuals and present-day populations. Outgroup f_3 statistics with topology of (MbutiPygmy; ancient individual, modern individual). (Related to Figure 2)

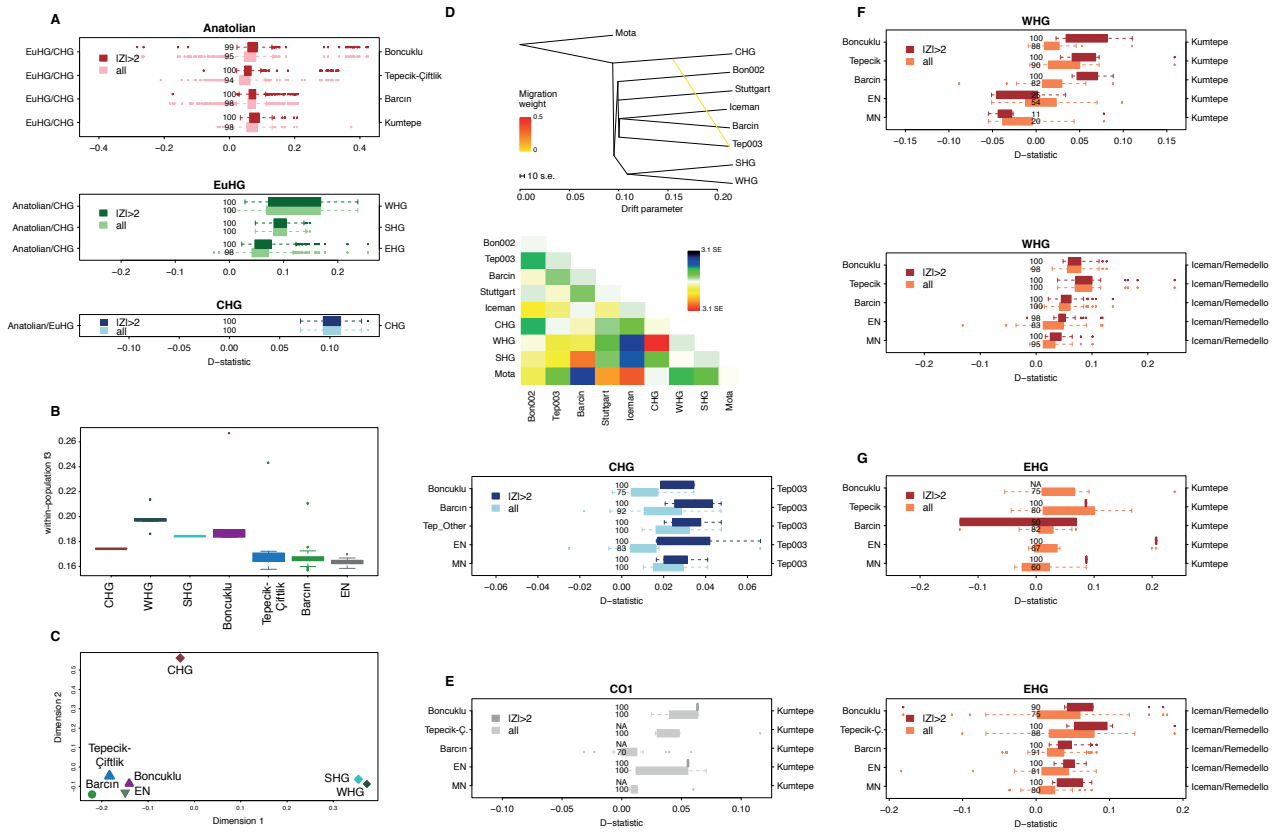

Figure S3. Genetic affinities between different populations (A) Boxplots of D-statistics for the topology *D(Denisova,Anatolian1;Anatolian2,Other)*, where Anatolian1 and Anatolian2 are two ancient Anatolian individuals and Other represents a European or Caucasus hunter-gatherer (CHG) individual; the topology *D(Denisova,EuHG1;EuHG2,Other)* where EuHG1 and EuHG2 are two European hunter-gatherer individuals, including Western European (WHG), Scandinavian (SHG), Eastern European hunter-gatherers (EHG), while Other represents a CHG or an ancient Anatolian individual; and the topology *D(Denisova,CHG1;CHG2,Other)* where CHG1 and CHG2 are two CHG individuals, while Other represents a European hunter-gatherer or an ancient Anatolian individual. In each comparison, boxplots show all D-statistics based on all available individuals in all populations (lighter colors), or only nominally significant D-statistics with $|Z|\geq 2$ (darker colors). The numbers in the middle indicate the percentage of comparisons where the test population resembles the population indicated on the right-hand y-axis. **(B)** Boxplots show within-population f_3-statistics for each population. Boncuklu had significantly higher within-population f_3 compared to both Tepecik-Çiftlik and Barcın (Mann-Whitney U test $p<0.01$ and 100% jackknife support). **(C)** Multidimensional scaling analysis based on mean f_3-statistics across populations. **(D)** TreeMix plot of the Tep003 with known migration from CHG model. **(E)** Boxplots of D statistics for the topology *D(Denisova,CO1;X,Kumtepe)* **(F)** Boxplots of D statistics for the topology *D(Denisova,WHG;X,Kumtepe)* and *D(Denisova,WHG;X,Iceman/Remedello)* **(G)** Boxplots of D statistics for the topology *D(Denisova,EHG;X,Kumtepe)* and *D(Denisova,EHG;X,Iceman/Remedello)*, where *X* stands for an ancient Anatolian or European early Neolithic (EN) or middle Neolithic (MN) individual, indicated on the left side y-axis. Results are plotted as in Panel A. (Related to Figure 2 and Figure3)

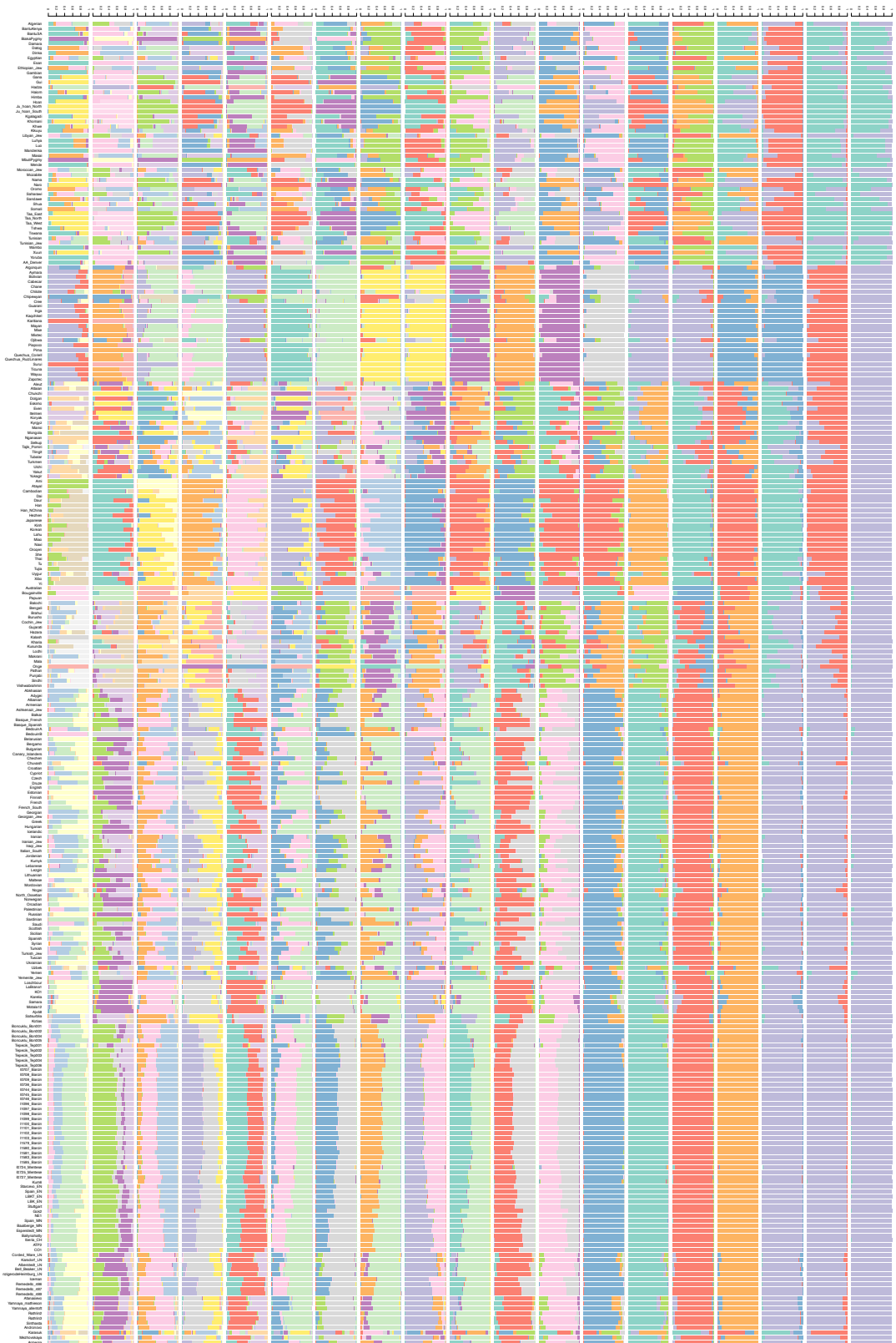

Figure S4. Admixture Analysis for K=2 to K=20. (Related to Figure 3)

Table S1: Number of SNPs of the ancient individuals used in this study, overlapping with reference datasets, either Human Origins ("HO") or the 1000 Genomes datasets. "Origin" refers to the population identity also used in Figure 2A. (*: this study). (Related to Figure 2)

Sample	Origin	HO	1000 Genomes	Source
Bon001	Boncuklu	24574	257166	*
Bon002	Boncuklu	356862	1750526	*
Bon004	Boncuklu	36263	353318	*
Bon005	Boncuklu	6459	70205	*
Tep001	Tepecik-Çiftlik	5193	45098	*
Tep002	Tepecik-Çiftlik	103179	765738	*
Tep003	Tepecik-Çiftlik	190517	872166	*
Tep004	Tepecik-Çiftlik	90488	582655	*
Tep006	Tepecik-Çiftlik	41142	393955	*
Denisova		389964	1845060	[S4]
Ust_Ishim		377273	1868221	[S5]
Oase1		75825	83498	[S6]
K14		244416	1037211	[S7]
MA1		132665	548352	[S8]
Bichon		379982	1827072	[S9]
Satsurblia		276697	1250908	[S9]
Kotias		378827	1812975	[S9]
Loschbour		378127	1869945	[S10]
LaBrana1		362114	1556281	[S11]
I0061	Karelia	353286	429688	[S12]
I0124	Samara	187268	111172	[S12]
KO1		257727	1125607	[S13]
Motala12		340648	1579528	[S10]
Ajv54		225442	1023721	[S14]
Ajv58		334932	1525594	[S14]
Bar8	Barcın	370414	1781411	[S15]
Bar31	Barcın	344306	1629480	[S15]
I0707	Barcın	352066	486817	[S12]
I0708	Barcın	343474	427669	[S12]
I0709	Barcın	348904	480918	[S12]
I0724	Mentese	22749	11743	[S12]
I0725	Mentese	14488	9037	[S12]
I0727	Mentese	15130	13826	[S12]
I0736	Barcın	305240	242288	[S12]
I0744	Barcın	314776	288254	[S12]
I0745	Barcın	351351	510681	[S12]
I0746	Barcın	352478	490715	[S12]
I1096	Barcın	262224	164676	[S12]
I1097	Barcın	260420	162100	[S12]
I1098	Barcın	274329	178294	[S12]
I1099	Barcın	186654	105584	[S12]
I1100	Barcın	99738	50128	[S12]
I1101	Barcın	228521	136845	[S12]
I1102	Barcın	138674	72212	[S12]

Sample	Origin	HO	1000 Genomes	Source
I1103	Barcın	208469	116473	[S12]
I1579	Barcın	279212	222938	[S12]
I1580	Barcın	312343	345227	[S12]
I1581	Barcın	280346	237593	[S12]
I1583	Barcın	335847	430493	[S12]
I1585	Barcın	283232	258647	[S12]
Kum6	Kum6	42069	179010	[S16]
I0174	Starcevo	93297	70796	[S12]
I0412	Spain	361180	670935	[S12]
I0176	LBKT	28641	21171	[S12]
I0100	LBK	351556	451996	[S12]
Stuttgart		377721	1849865	[S10]
Gok2		264828	959786	[S14]
ne7		234554	1026839	[S13]
ne1		375720	1850494	[S13]
I0408	Spain_MN	351352	498932	[S12]
I0560	Baalberge	141097	128812	[S12]
I0172	Esperstedt	371104	996699	[S12]
Ballynahatty		376668	1825174	[S17]
Iceman		373241	1528382	[S18]
I1300	Iberia	277445	196493	[S12]
ATP2		364082	1724404	[S19]
CO1		220323	967387	[S13]
I0103	Corded_Ware	368046	768507	[S12]
I0550	Karsdorf	62091	65070	[S12]
I0118	Alberstedt	367883	646574	[S12]
I0112	Bell_Beaker	343500	403502	[S12]
I0058	Benzigerode Heimburg	165158	56117	[S20]
RISE486	Remedello	60707	238049	[S21]
RISE487	Remedello	54117	234503	[S21]
RISE489	Remedello	150615	601768	[S21]
RISE508	Afanasievo	85966	252282	[S21]
I0231	Yamnaya_M	364439	667074	[S12]
RISE552	Yamnaya_A	327310	1208368	[S21]
Rathlin2		293436	1317947	[S17]
Rathlin3		206612	905407	[S17]
RISE395	Sinthasta	316486	1173415	[S21]
RISE505	Andronovo	367868	1611645	[S21]
RISE497	Karasuk	375986	1663555	[S21]
RISE523	Mezhovskaya	338921	1249961	[S21]
RISE423	Armenia	135554	508622	[S21]
RISE600	Iron Age	160309	720433	[S21]
Mota		384394	1831580	[S22]

Supplemental Experimental Procedures

Archaeological context of the samples

Neolithic on the Anatolian plateau

The Anatolian plateau, along with the Fertile Crescent, has been a major focus of Neolithic studies. The plateau can be divided into several geomorphological and cultural subregions: the Salt Lake region, the Konya Plain, Volcanic Cappadocia, and Sultansazlığı. The Epipalaeolithic of the plateau and its coastal fringes is poorly documented [S23]. However, one site on the plateau has been excavated at Pınarbaşı in the Konya Plain, where unlike the partially contemporary Levantine Early Natufian, there is no evidence of sedentary practices or intensive plant exploitation [S24]. The earliest sedentarising communities on the plateau appear in the 10th-9th millennia cal BC and are represented also by occupation at Pınarbaşı which lacks evidence of cultivation or herding [S25].

The Pre-Pottery Neolithic period (PPN) of the plateau is better understood. Among the human groups and cultures of the Konya Plain there are indications of highly diverse but indigenous communities during this phase of uptake of sedentism, of cultivation and of herding. Boncuklu and Aşıklı Höyük Level 4 [S26,27] have the earliest evidence of cereal and legume cultivation detected to date on the plateau. At both sites it was present by c. 8300 cal BC, presumably appearing somewhat earlier, but apparently post-dating the development of cultivation in the northerrn Levant, where cultivation appeared during the course of the10th and early 9th millennia cal BC. Substantial evidence of herding of morphologically wild sheep and goat (caprines) is present at Aşıklı also by 8300 cal BC [S28]. Sub-oval mud-brick houses characterise Boncuklu and early phases at Aşıklı Höyük in the second half of the 9th millennium cal BC. They are replaced by rectilinear closely packed house clusters in later phases at Aşıklı Höyük [S29] and Canhasan III [S30] in the 8th millennium cal BC. In the same period, the obsidian sources of Göllüdağ inVolcanic Cappadocia provide a focus for both settlement and those exploiting the sources for exchange, as obsidian from the region was exported to North Mesopotamia and the Levant, as well as Cilicia and Cyprus [S31]. There is thus substantial evidence for interactions between central Anatolia, the south coast of Turkey, the Levant and areas south-east of the Taurus from the Epipalaeolithic into the Pottery Neolithic [S32]. Several PPN sites have been discovered around and not far from the Göllüdağ obsidian beds and workshops. The variation in settlement types is remarkable; scattered site clusters like Yapılıpınar/Çakılbaşı, flat settlements with single period occupations, camp sites on scoria cones, rock shelters. The only stratified mound site Tepecik-Çiftlik has PPN levels in its lower strata [S33].

A diversity of cultures can be described in the Anatolian plateau during the subsequent Pottery Neolithic, considered to span from c.7000 to c.6000 cal BC. In Çatalhöyük in the Konya Plain [S34,35] we find rectilinear closely packed house clusters as at 8th millennium Aşıklı Höyük, and domestic organization that resembles 9th-8th millennium Boncuklu. In contrast, Tepecik-Çiftlik and Köşk Höyük in Volcanic Cappadocia have independent houses and open areas, pointing to cultural differences with the Konya plain. In the Pottery Neolithic, the Volcanic Cappadocia region still contains many workshops for obsidian tools and weapons. Recent work has detected many new settlements in the Volcanic Cappadocia region; these are thought to be related to migrating individuals and small groups, possibly moving over quite significant distances, attracted by the local obsidian sources [S32]. Finally, in the cultural/geomorphological region Sultansazlığı PPN and Pottery Neolithic sites are known only from surveys. The locations of the settlements on the dunes, hilltops and small valleys around the Holocene lake resembles those of Konya Plain.

Boncuklu

The site of Boncuklu is a small archaeological settlement mound in the northern part of the Çarşamba fan in the south-west Konya basin. The probable span of occupation was 8300-7500 cal BC. The site consists of a series of sub-oval structures with mudbrick superstructures; and extensive intervening open areas [S26]. Buildings have relatively standard domestic features and a highly structured use of domestic space, divided into ‘clean’ and ‘dirty’ areas. Buildings are also reconstructed over a number of generations in the same place, standing as a symbolic testament to the endurance, and social, economic and reproductive success of the household. At Boncuklu the evidence indicates adoption of cultivation by indigenous foragers, sometime before 8300 cal BC [S23]. This interpretation is based on continuities in very specific local technological practices and symbolism in the area and which are seen already c. 9500 cal BC and thus predate domestic plants in the Konya Plain by 1000 years [S26]. These plants were presumably introduced to the plain in the first instance as part of the far-reaching interactions in the 10^{th} and 9^{th} millennium, which have been documented at earlier and contemporary Pınarbaşı, as well as Boncuklu itself. Burials occur at Boncuklu under the ‘clean’ south-eastern areas in houses but in the open spaces between houses as well. All the burials under the houses are complete articulated inhumations, as are many of

those in the open areas. However, there is evidence of secondary mortuary practices on the site, with the burial of partial articulated remains and the circulation and deposition of skulls in the open areas [S26]. All of these human remains are thus well stratified within the settlement in relation to buildings, midden deposition and thus each other.

Tepecik-Çiftlik

Tepecik-Çiftlik is located in the Melendiz/Çiftlik Plain which is surrounded by the Melendiz Volcanic Mountains, lying along the southwest of the Volcanic Cappadocia region and the southern part of Central Anatolia [S33]. The occupation at the settlement probably continued uninterrupted from the Aceramic Neolithic Period until the early Chalcolithic Period, i.e. between 7500-5800 cal BC. The presence of yet unexcavated levels shows that the initial date of the settlement at the höyük predates 7500 BC. The Aceramic Neolithic levels do not contain architectural remains. In the Pottery Neolithic levels (5-4) the settlement layout consisted of wide open areas and single large structures but in the final Neolithic level (3) the settlement layout changed as the open areas were replaced by different types of structures. Utilization of domestic animals occurred in the Neolithic period at Tepecik-Çiftlik but hunting of wild fauna was still practiced and during the end of the Neolithic Period hunting, in fact, gained significance in the subsistence. During the Neolithic Period, alongside agriculture, intensive gathering also continued. The pottery at Tepecik-Çiftlik is the oldest in the region and of significant importance is its closeness to the Göllüdağ and other obsidian ore beds in the region. Obsidian as a raw material played a significant role in all of Near East and during the entire Neolithic Period for tools and arms production and there was a demand for obsidian tools and arms in many areas [S31]. Intensive obsidian tool production occurred at Tepecik-Çiftlik and also other Volcanic Cappadocia sites such as Yapılıpınar, Çakılbaşı, "Kayırlı Girişi/Sapağı", Bunuş and Nuzla. The obsidian tool and arms production "industry" in the region may have resembled "commodity" production [S33].

During archaeological fieldwork, a large number of human burials have been unearthed, beginning from the 5th level of the stratigraphy. The single and multiple burials dated to the Neolithic the number of the individuals is over 170. Beside primary and secondary burials, there are skull burials and also numerous individuals without skulls. Most of the graves contain single primary burials while most of the secondary burials contain bones of multiple individuals. A significant number of individuals were buried in hocker (crouched) positions, on their left or right sides with varying body orientations. The Neolithic graves are found in the courtyards, inside of the buildings and in open areas. However, a mass grave called BB was revealed in the 5th level. Among the individuals retrieved from this collective burial site are females and males of all age groups (i.e. infants, children, young adult) except for very young infants. The unique burial contains bones of at least 42 individuals. The general characteristics of the mortuary practices at Tepecik-Çiftlik are characteristic of the Aceramic Neolithic of the Near East [S36].

Sample description

Boncuklu individuals

The four individuals, subject to aDNA analysis in this paper, with context codes ZHF, ZHB, ZHBJ, ZHAF, (Data set 1) were all articulated single inhumations buried in oval cuts and stratified within the settlement sequence at the site. It should be noted that all four individuals were buried in one small part of the site, closely related to a sequence of buildings in that area. ZHB was directly dated to the last quarter of the 9th millennium cal BC by C14: range 8279-7977 cal BC (Oxcal) 2 sigma at 95.4% probability (lab number Wk29763). ZHF was dated to a similar time frame: range 8212-7952 cal BC (Oxcal) 2 sigma 95.4% probability (lab number BA120539). ZHAF was dated by C14 to 8300-8240 cal BC (Oxcal) 2 sigma 95.4% probability (lanb number WK43898). The other burial predates these directly dated individuals. Adult individuals were assigned to three age categories: young, middle and old. Young adults were individuals aged approx. 20-30, mature adults were aged approx. 30-50 and old adults were those over 50 years. Since adult age is dependent upon degenerative changes to the skeleton, these ages are approximate stages and should not be considered as exact numerical figures or directly comparable to calendar years.

ZHF Grave 14 (Bon001): A single inhumation of an adult individual. Key elements were not sufficiently preserved to estimate an age more precisely. Morphology was inconclusive, however the genetic analysis indicates it is a male. The individual was found lying on its left side in a tightly flexed position.

ZHB Grave 9 (Bon002): Single inhumation of a young to middle age category adult female. The individual was lying on their right side and partially prone, in a lightly flexed position. Genetic analysis confirms the assignation to sex made on morphological grounds.

ZHBJ Grave 30 (Bon004): A single inhumation of a middle-old age category adult male. The individual was found lying tightly flexed on their side. Genetic analysis confirms the assignation to sex made on morphological grounds.

ZHAF Grave 18 (Bon005): A middle age category adult female lying on her left side in a tightly flexed position. She was accompanied by a perinatal baby not analysed here. The arrangement of the skeletal remains was quite distinct with the perinatal child placed at one end of the grave. Genetic analysis confirms the assignation to sex made on morphological grounds.

Tepecik-Çiftlik individuals

TP'10 BB 4-23 (*Tep001*): This male individual is estimated to be a young adult (nearly 25-30 years old). The morphological sex assessment is in agreement with the genetic analysis. The individual comes from the 5th level of Tepecik-Çiftlik settlement and was obtained from BB collective burial. He is one of the few primary burials identified in BB collective burial. Whereas the upper side of this individual was laid down on his back in south-north direction, legs were positioned on his left side in crouched form.

TP'10 SK 40 (*Tep002*): The individual is represented by a mandible. Although the exact age could not be determined, it can be said that it belongs to an adult individual. Genetic analysis indicates that the individual was female. The burial SK 40 is located in fifth level of the settlement and was found at a very close location to BB collective burial. It is a secondary multiple burial and has different types of bones presenting at least four people.

TP'09 16 K (*Tep003*): The individual is presented by some parts of the skull. Although the exact age could not be determined, it can be said that it belongs to an adult individual. According to the genetic analysis the individual is male. The partial skull was found in 16 K sounding area of the settlement during the 2009 excavation season and it belongs to fifth level of the settlement.

TP'10 SK 37 (Tep004): The remains of this adult individual were in bad condition, so the exact age could not be determined. The sex of this individual estimated by osteological techniques is female which is in agreement with genetic data. The burial comes from the fourth level of the settlement. She is one of the individuals obtained from the western part of the AY room, part of the larger AK building complex. The individual has north-south direction, laid down on her left side and in a crouched position. In the grave there were various post-cranial disarticulated bones belonging to a different individual. The stratigraphy shows that SK37 is of earlier date than the other burials in room AY.

TP'10 SK 21 (Tep006): Osteological analysis indicates that this is an elderly individual (nearly 45-50 years old). According to osteological analysis the individual is male which was confirmed by genetic data. Antemortem tooth loss was observed for all the teeth together with various degrees of osteoarthritis in long bones and trunk bones. The burial comes from fourth level of the settlement in the eastern part of room AY, part of the larger building complex AK. The individual has a southeast-northwest direction, laid down on his right side and in a crouched position. In the grave there were various post-cranial disarticulated and articulated bones belonging to different individuals. Two potsherds were found as grave goods.

Sample preparation

Sample preparation, DNA extraction and library preparation from 4 Boncuklu and 5 Tepecik-Çiftlik samples were carried out in a laboratory dedicated to ancient DNA at the Middle East Technical University. Teeth and bone samples were decontaminated as in [S37]: The outer surface of the bone or teeth were removed using a single use blade. Teeth were wiped with 5% sodiumhypochlorite (NaClO) and then rinsed with nuclease free water. Each sample was placed in a petri dish and UV-irradiated (254 nm wavelength, 12 V and a distance of 5 cm from the UV source) in a cross-linker for 60 minutes from two sides. The bones were ground into fine powder using freezer mill.

DNA Extraction

Two different protocols were used for DNA isolations [S37,38]. In the first protocol, DNA extraction from 300 mg bone powder was performed with slight modifications based on [S37]. Bone powder was mixed with 1608 µl of lysis buffer (0.5 M EDTA pH 8, 20 mg/ml Proteinase K) and incubated in a shaker incubator first at 56 ^{0}C for 24 hours, then at 37 ^{0}C for 24 hours. DNA extraction was completed using silica spin columns, with a final elution of 104 µl. Two blank extractions were also carried out; for the grinding blank we used hydroxyapatite instead of bone powder. In the second protocol, 80-150 mg bone powder was mixed with extraction buffer (0.45 M EDTA pH8, 0.25 mg/ml Proteinase-K) and incubated for at least 18 hours at 37 ^{0}C in a shaker incubator and then centrifuged to obtain supernatant. 13 µl binding buffer (5 M Guanidine Hydrochloride, 40% (vol/vol) Isopropanol, 0.05% Tween-20, 90mM Sodium Acetate) was added to the supernatant. This mixture was filtered through Qiagen PCR Minelute spin columns to bind and wash the DNA, which was eluted with 48 µl of Qiagen Elution Buffer.

Library preparation

Double stranded DNA libraries were prepared using 20 µl of extract, with blunt-end ligation as described in [S39] with modifications as in [S19]. The initial nebulization step was omitted since aDNA is already fragmented. Each library was amplified in six replicates, each in a total volume of 25 µl. Two negative controls were included in each PCR batch. Each reaction contained 3 µl DNA library and the following in final concentrations; 1X AmpliTaqGold Buffer, 2.5 mM $MgCl_2$, 250 nM of each dNTP, 2.5U AmpliTaqGold (Life Technologies), and 200 nM each of the IS4 primer and an Indexed P7 primer. The cycling conditions were 94 C° for 10 min followed by 10-14 cycles of 94 C° for 30 sec, 60 C° for 30 sec, 72 C° for 45 sec, and a final extension at 72 C° for 10 min. Amplified libraries were pooled and purified with AMPure XP beads (Agencourt). The libraries were quantified on a 2100 Bioanalyzer using the High Sensitivity Kit (Agilent Technologies). None of the extraction blanks or PCR blanks showed presence of DNA and were therefore not further sequenced.

Initial sequencing

Libraries were pooled at equimolar concentrations for initial screening process. Sequencing was done on Illumina HiSeq 2500 and HiSeq X platforms at the SNP & SEQ Technology Platform at the Science for Life laboratory, Stockholm University. Each pool was sequenced with version 3 chemistry and 100 bp paired-end reads on one or several lanes. Libraries that yielded sufficient reads from the initial screening process were then selected and sequenced deeper in pools of four to six libraries per lane.

Whole genome in-solution capture and resequencing

In order to increase the depth of coverage, all the libraries built from the samples Bon001, Bon002, Bon004, Bon005, Tep001, Tep002, Tep003, Tep004, and Tep006 (Data set 2) were enriched using the MYbait Human Whole Genome Capture Kit from MYcroarray (Ann Arbor, MI). The libraries were captured following the manufacturer's instructions (http://www.mycroarray.com/pdf/MYbaits-manual-v3.pdf). The captured libraries were amplified for 10–19 cycles using primers IS5 (5' AATGATACGGCGACCACCGA) and IS6 (5' AAGCAGAAGACGGCATACGA) and Herculase II Fusion DNA Polymerase (Agilent Technologies). Subsequently, libraries were purified with AMPure XP beads and quantified by 2100 Bioanalyzer (Agilent Technologies). Purified libraries were pooled in equimolar amounts and sequenced on HiSeq 2500 and HiSeq X.

Processing of the ancient genome sequence data

We performed base calling using Illumina CASAVA software and de-multiplexed the sequences by requiring a complete match with the 6-nucleotide index sequences used in library preparation. Using MergeReadsFastQ_cc.py [S40], we removed the residual adapter sequences in FASTQ files and merged the paired-end sequencing reads with a requirement of minimum 11 bp overlap between the pairs. We mapped the merged reads to the human reference genome (version hs37d5 and hg18) using BWA [S41] version 0.7.12 in single-end mode with parameters -n 0.01 -o 2 and disabled the seed with –l 16500 as reported in [S10,14]. We merged the data from libraries of each individual and collapsed the PCR duplicates with identical start and end coordinates using FilterUniqueSAMCons.py [S40]. We filtered reads with length of less than 35 bp and required less than 10% mismatches to the human reference genome for each read. For comparative analysis, we re-mapped the published ancient data from individuals in Table S1, using the same procedure. We evaluated the success rate of using either teeth or petrous bone samples with respect to the endogenous DNA content (Figure S1A, Data set 2). We calculated the mean endogenous DNA content and clonality for each sample across libraries to compare the efficiency of sequencing in whole genome capture and non-capture libraries (Figure S1B).

Estimation of the contamination and authentication of data

To evaluate the authenticity of the genomes, we used a set of well-established approaches including the a) examination of ancient DNA specific damage patterns, b) X-chromosome-based contamination estimation in males, and c) mtDNA-based contamination estimation in all samples.

We first assessed the aDNA-specific DNA damage patterns that are not expected to be present in modern-day human DNA: high frequency of the cytosine to thymine (C to T) transitions at the 5' end of DNA due to cytosine deamination and short fragment length due to DNA strand breaks [S42,43]. We used PMDtools to evaluate the nucleotide misincorporation patterns at the first 30 positions at the 5' ends of the reads [S44]. All sequence data showed evidence of elevated C to T substitution frequencies at the ends of the DNA molecules (between 32%-24% at the first 5' base (Figure S1C). Mean read length of data ranged between 52-84 nucleotides.

We estimated the DNA contamination fractions using different approaches that are based on the examination of polymorphic positions in mitochondrial and X chromosomes in all samples and in males, respectively. In the first method, we obtained mitochondrial DNA contamination estimates using the approach adopted in [S16]. Here we first identified the private or near-private consensus alleles (<5 % in 311 modern mtDNA sequences) with minimum depth of 10X and minimum base quality of 30 in ancient individuals. We filtered positions where the consensus allele is C or G and a transition type substitution were detected, to prevent confounding with postmortem damage. We obtained the point estimate of mtDNA contamination by adding the counts of consensus and alternative nucleotides across all sites. For one of the nine samples (Tep001) we could not obtain the contamination estimates using this method, due to lack of informative sites with sufficient coverage. For the remaining 8 individuals average proportion of contamination ranged between 0.6% and 7.9% with a median of 1% (Data set 1). In the second method, we calculated the posterior probability of mtDNA contamination using a Bayesian approach described in [S1]. In brief, we called a consensus sequence for the samples using mpileup and vcfutils modules of the samtools [S45], and mapped the consensus sequences to a set of 311 modern human mtDNA sequences. Using contamMix, we calculated the probabilities of the authenticity for all samples (Data set 1). All individuals passed minimum one of the two mitochondrial DNA based contamination estimations. In the third method, for all male individuals in our study, we estimated the rate of contamination using a maximum likelihood method described in [S46] and implemented in the ANGSD (http://www.popgen.dk/angsd/) package (Data set 1). Given limitations in specificity and sensitivity of each of the above approaches, we assessed the results in combination, to ensure that none of the ancient individuals investigated here failed more than one contamination estimation method. Based on these results and post-mortem damage and read length analyses, we included all samples in further population genetics analysis.

Mitochondrial haplogroups

We obtained mtDNA sequence with mean coverage between 66- and 2,379-fold per individual. From this data, we called consensus mitochondrial sequences of each individual using the mpileup and vcfutils.pl (vcf2fq) tools in the samtools package with default parameters [S45]. We determined the mitochondrial DNA haplogroups of the individuals based on SNPs at informative nucleotide positions of the mitochondrial genome sequences (Data set 2). For this, we aligned mtDNA sequence of each individual to the RSRS [S47], identified the polymorphisms and analyzed these using HaploFind and PhyloTree [S48,49]. To prevent possible misinterpretation that might arise due to classification of missing sequences as deletions in HaploFind, we examined each consensus manually.

We observed haplogroup N1, the most abundant haplogroup in Neolithic farmer populations [S50], in five individuals from Central Anatolia. Four belonged to subtypes of N1a (N1a1a1) and one, from Tepecik-Çiftlik, belonged to N1b (N1b1a). One individual from Boncuklu belonged to U3. The remaining three individuals from Central Anatolia belonged to another common haplogroup in Neolithic farmer populations, K (K1a, K1a and K1a12a).

The Bon001 mitochondrial genome has 46 mutations classifying it as haplogroup U3 (Data set 2). 19 additional mutations were found in the consensus sequence, and 14 of these were C to T or G to A transitions attributable to post-mortem damage [S51]. The Bon002 mitochondrial genome has 50 mutations classifying it as haplogroup K1a (Data set 2). Six additional mutations (5 of these C to T or G to A) were found in the consensus sequence. The Bon004 mitochondrial genome has 49 mutations classifying it as haplogroup N1a1a1 (Data set 2). 20 additional mutations (16 of these C to T or G to A) were found in the consensus sequence. The Bon005 mitochondrial genome has 48 mutations classifying it as haplogroup N1a1a1 (Data set 2). 34 additional mutations (33 of these C to T or G to A) were found in the consensus sequence. The Tep001 mitochondrial genome has 48 mutations classifying it as haplogroup K1a (Data set 2). 36 additional mutations (35 of these C to T or G to A) were found in the consensus

sequence. The Tep002 mitochondrial genome has 53 mutations classifying it as haplogroup K1a12a (Data set 2). Eleven additional mutations (9 of these C to T or G to A) were found in the consensus sequence. The Tep003 mitochondrial genome has 52 mutations classifying it as haplogroup N1b1a (Data set 2). 16 additional mutations (15 of these C to T or G to A) were found in the consensus sequence. The Tep004 mitochondrial genome has 51 mutations classifying it as haplogroup N1a1a1 (Data set 2). 23 additional mutations (20 of these C to T or G to A) were found in the consensus sequence. The Tep006 mitochondrial genome has 52 mutations classifying it as haplogroup N1a1a1 (Data set 2). 14 additional mutations (12 of these C to T or G to A) were found in the consensus sequence.

Haplogroup N1a is typical of early European farmer from the Linearbandkeramik (LBK) culture of Central Europe. Haplogroups K and N1a are characterized as Early and Middle Neolithic [S50]. Both of these haplogroups were frequently observed in Barcın, LBK, LBKT (Linearbandkeramik culture in Transdanubia, 5800–4900 BC), STA (Early Neolithic Starčevo culture, 6000–5400 BC) populations including four Central European Neolithic groups (RSC, SCG, BAC and SMC) [S12,50,52]. K1a is common in present day Near East (Levant) and in Europe [S53], while N1 is described to be common in modern-day West Eurasia [S54]. The European hunter-gatherers mostly carried haplogroup U lineages including U, U2, U4, U5 and U8 [S2,50,55]. Meanwhile, U3 was not detected among Mesolithic individuals, and it is unclear whether there was a Mesolithic or a Neolithic emergence of haplogroup U3 in Central Europe [S50,56]. We constructed an mtDNA haplogroup network for 9 individuals using Network v5 (http://www.fluxus-engineering.com) (Figure S1D).

Biological sex determination

To determine the biological sex of all individuals, we used the R_y method as described in [S57,58]. In short, we used reads with mapping quality of minimum 30 and calculated the ratio of reads mapping to the Y chromosome to those mapping to both X and Y chromosomes. 5 individuals were assigned as males and 4 individuals were assigned as females (Data set 1).

Population genetics analysis datasets

We prepared two different datasets (to be used in different population genetics analyses) by merging the ancient sequence data produced in this study with ancient genome data from previous studies (Table S1) and with two different genotype datasets of contemporary individuals including i) Human Origins SNP Array and ii) 1000 Genomes whole genome sequencing datasets.

Human Origins SNP Array dataset

We obtained a curated version of Human Origins SNP Array dataset which includes 594,924 autosomal SNP genotype calls for 2,730 modern-day individuals from 203 different populations and 14 ancient individuals from [S10,59]. To merge ancient individuals with this dataset, we identified all reads with base quality and mapping quality of 30 or higher, and with overlapping positions with the Human Origins dataset. Whenever multiple reads overlapped with the same position, we randomly selected one read, and thus haploidized our data as in [S19]. We discarded all sites where an ancient individual carried an allele not found in the reference data, as well as all transitions and indels.

1000 Genomes dataset

We downloaded VCF and BAM files of African Yoruba individuals (n=108) from phase 3 of the 1000 genomes project from ftp.1000genomes.ebi.ac.uk [S60]. We used Yorubans as ascertainment population, for which we have good quality genomic data and who are known to be essentially isolated from Eurasian populations [S14]. We filtered the dataset by extracting all transversion SNPs with a minor allele frequency of 10% in African Yoruba population using vcftools [S61]. A total of 1,938,919 SNPs remained. We merged ancient genomes with these SNPs as described above.

Principal component analysis

We conducted principal component analysis (PCA) using a subset of individuals from the Human Origins SNP Array dataset. For PCA, we used a total of 55 modern West Eurasian populations and 85 ancient individuals (76 previously published and 9 reported here). We haploidized the dataset by randomly selecting a single allele at each heterozygous site for all the modern-day individuals, as in [S16,19]. We performed PCA of the modern-day

individuals using the smartpca program of EIGENSOFT [S62] with numoutlieriter: 0 and lsqproject: YES options, and projected the ancient individuals onto the first two principal components inferred from modern individuals. We plotted the result using the ploteig program of EIGENSOFT [S62].

ADMIXTURE analysis

We carried out unsupervised clustering using the algorithm ADMIXTURE [S63], where we estimated ancestry components using contemporary Eurasian, African, Asian, and American groups from the Human Origins dataset [S10,59], and used these components to cluster the ancient genomes. Prior to ADMIXTURE analysis, we filtered the Human Origins Array dataset for linkage disequilibrium using PLINK [S64], with parameters --indep-pairwise 200 25 0.4. This filtering resulted in a total of 293,404 SNPs. We conducted ADMIXTURE analysis as described in [S65]. In brief, we determined ancestral clusters for modern-day populations using ADMIXTURE and inferred the cluster memberships of each ancient individual using the ancestral allele frequencies. Therefore, ancient samples did not have influence on ancestral clusters and the difference in number of overlapping SNPs across samples did not interfere with the results.

We determined the cluster memberships of each ancient individual through maximization of the following log-likelihood function, an adapted version of Eqn2 in [S63]:

$$L(Q,F) = \sum_i g_i \ln\left(\sum_k (q_k f_{ik})\right) + (2-g_i)\ln\left(\sum_k q_k(1-f_{ik})\right)$$

where;

g_i : genotype at the position *i*

q_k : contribution of population *k* to a sample

f_{ik} : frequency of a variant at position *i* in population *k*. These values are obtained from the output of ADMIXTURE that was run on modern individuals.

The optimization was implemented through the following formula which was defined as a part of FRAPPE EM algorithm in [S63]:

$$q_k^{n+1} = \frac{1}{2I}\sum_i g_i a_{ik}^n + (2-g_i) b_{ik}^n$$

$$a_{ik}^n = \frac{q_k^n f_{ik}^n}{\sum_m q_m^n f_{im}^n} \text{ and } b_{ik}^n = \frac{q_k^n (1-f_{ik}^n)}{\sum_m q_m^n (1-f_{im}^n)}$$

$$L(Q^{n+1}, F^{n+1}) - L(Q^n, F^n) < \epsilon$$

$\epsilon = 10^{-4}$ was used as the convergence criteria, as implemented in the original ADMIXTURE software.

We performed clustering of the modern individuals as well as the ancient individuals between K=2 and K=20 (Figure S4). For each K, we carried out 50 replicate runs with different random seeds for each modern individual and determined the clusters of each ancient individual. We identified common signals between different replicates for each K using LargeKGreedy algorithm of CLUMPP [S66]. We compared cluster proportions between ancient populations using one-sided Mann-Whitney U tests in R.

Outgroup-*f3* statistics

We used outgroup-*f3* statistic to evaluate the genetic relationship between two populations regarding the shared genetic drift between them since their divergence from a common ancestral population. This statistic is not affected by an excess of drift in either of the populations [S59]. We calculated the statistic as in the formula:

$$f3(O;A,B) = \frac{\Sigma(p_o - p_A)(p_o - p_B) - (p_o - p_O^2)/(n_O - 1)}{\Sigma 2 p_O (1 - p_O)}$$

where;

p_O: allele frequency of the reference allele.

n_O: number of chromosomes in outgroup populatin (O) at locus i.

We used Mbuti Pygmy (in comparisons with modern populations in the Human Origins dataset) or Yoruba (in comparisons with ancient individuals, to maximize the number of overlapping SNPs) as outgroup. A positive value of this statistic indicates the shared genetic drift between populations A and B. For Figure S3C, we converted f3 statistics into a distance measure by subtracting all values from 1, and summarized these values by multidimenstional scaling (MDS) using the *cmdscale* function of R.

D-statistics

We carried out formal tests of admixture using D-statistics to investigate relationships between ancient individuals. We tested deviations from a tree-like population topology by computing D-statistics implemented in ADMIXTOOLS qpDstat program [S59], based on:

$$D(A,B;X,Y) = \frac{\sum_{i=1}^{n}[S(p_{iA}-p_{iB})(p_{iX}-p_{iY})]}{\sum_{i=1}^{n}[S(p_{iA}+p_{iB}-2p_{iA}p_{iB})(p_{iX}+p_{iY}-2p_{iX}p_{iY})]}$$

where;

p_{iA}: frequency of a randomly chosen allele at marker *i* in population A.

n: total number of markers

We tested the significance of each test by computing standard errors using a block jackknife of 5cM in size. Significant deviations from zero indicates deviation from the proposed tree with topology (*A*,*B*)(*X*,*Y*). When A is the outgroup, positive values indicate that the population B is closer to population Y; while negative values shows that the population B is closer to population X. We used the high-coverage Denisovan genome [S4] as outgroup in this analysis.

Conditional nucleotide diversity

We assessed within-population diversity by computing conditional nucleotide diversity as described in [S14,19]. In brief, the method is based on estimating the average number of mismatches for all sites between two individuals. Here we used two ancient contemporaneous individuals for each ancient population: Bon001 and Bon002 for Boncuklu; Tep002 and Tep003 for Tepecik-Çiftlik (both from level 5); Bar8 and Bar31 for Barcın [S15]; ne1 and ne7 (from Hungary) for European early Neolithics (EN) [S13]; Loschbour [S10] and LaBrana [S11] for western European hunter-gatherers (WHG); Kotias and Satsurblia for Caucasus hunter-gatherers (CHG) [S9]; Ajv58 and Ajv54 for Swedish hunter-gatherers (SHG) [S14]. We chose individual pairs to be close to each other with respect to their ages and have the highest number of SNPs. We restricted our calculation to transversion SNPs identified in Yorubans to prevent the possible effects of ascertainment bias as well as post-mortem damage. We tested the significance of results by calculating standard errors using block jackknife over blocks of 500 SNPs.

Weir and Cockerham's Fst estimation

We computed F_{st} as in [S14], using Weir and Cockerham's estimator, implemented in 'popstats' program (https://github.com/pontussk/popstats). We used transversion polymorphisms identified in Yorubans as described earlier. F_{st} estimates for all populations were computed with two ancient individuals – same with those used in diversity estimates. We conducted MDS analysis based on F_{st}, using *cmdscale* function of R.

Admixture graph inference

We inferred the relationships amongst ancient populations in the form of a bifurcating tree, using a statistical framework implemented in TreeMix [S67]. Treemix builds a maximum likelihood tree of populations and fit admixture edges to given populations using the covariance matrix of allele frequencies. We applied TreeMix to Bon002, Tep003, I0745 (Barcın), Stuttgart, Iceman, Loschbour (WHG), Kotias (CHG), Motala12 (SHG) and Mota. Since we used a single individual as representative of each population, we turned off the correction for low sample size using "–noss" option. We rooted the tree with high coverage ancient Ethiopian Mota [S22] individual. We restricted the analysis to a total of 210,973 transversion SNPs genotyped in all ancient individuals, which were ascertained in African Yoruba individuals from the 1000 Genomes project. We fitted an admixture graph by modeling gene flow from CHG to Tepecik-Çiftlik population (observed in ADMIXTURE analysis and D tests), using the –cor-mig option of TreeMix. We determined the starting proportion of admixture as 0.0 to allow the 0% possibility of gene flow. We estimated the standard errors using blocks of 500 SNPs. We ran TreeMix in this setting with 50 different random seeds. Each of the runs supported the observed result. We plotted the resulting tree and residuals using the plotting functions provided Treemix.

Permutation test for population differentiation using f_3-statistics

We used a permutation scheme to test differentiation between two populations based on pairwise f_3 statistics, using the R environment. We first calculated all pairwise f_3 values of the type $f_3(Outgroup, IPop_1, IPop_2)$, where $IPop_1$ and $IPop_2$ stand for the n_1 and n_2 members of Pop_1 and Pop_2, respectively. We used the mean of these n_1*n_2 f_3 values as a measure of observed genetic similarity between Pop_1 and Pop_2. Next, for 10,000 times, we randomized group memberships, creating two groups again with n_1 and n_2 members and calculating mean f_3 for the randomized groups. These mean f_3 values represent the null distribution for no difference. Finally, we calculated a one-sided permutation test p-value for population differentiation by determining the number of times the observed mean f_3 is equal to or lower than the null expectation.

Jackknife resampling for comparing homozygosities using f_3-statistics

To confirm population homozygosity differences estimated using conditional nucleotide diversity, we used mean within-population pairwise f_3 values. We first tested difference in mean within-population pairwise f_3 values using the Mann-Whitney U test. To ensure that this result is not influenced by single individuals, we repeated the analysis leaving out one individual at a time, creating n=20 jackknife resamplings for Boncuklu vs. Tepecik-Çiftlik and n=80 jackknife resamplings for Boncuklu vs. Barcın comparisons.

Estimation of the runs of homozygosity

We analyzed four high coverage ancient genomes (Bon002, Barcın8, Loschbour and Stuttgart) for runs of homozygosity (ROH). The diploid genotype calling was performed using autosomal transversions from Yorubans in the 1000 Genomes phase 3 dataset [S60] with samtools mpileup [S45], which generated between 1,789,956 and 1,891,896 transversion SNPs for these four samples. We identified ROH as in [S17] using PLINK [S64] version 1.90 with parameters (--homozyg , --homozyg-window-snp 50, --homozyg-window-het 1, --homozyg-window-threshold 0.05, --homozyg-snp 50, --homozyg-kb 500, --homozyg-density 50, --homozyg-gap 100).

Supplemental References

S1. Green, R.E., Malaspinas, A.S., Krause, J., Briggs, A.W., Johnson, P.L.F., Uhler, C., Meyer, M., Good, J.M., Maricic, T., Stenzel, U., et al. (2008). A complete neandertal mitochondrial genome sequence determined by high-throughput sequencing. Cell *134*, 416–426.

S2. Fu, Q., Mittnik, A., Johnson, P.L.F., Bos, K., Lari, M., Bollongino, R., Sun, C., Giemsch, L., Schmitz, R., Burger, J., et al. (2013). A revised timescale for human evolution based on ancient mitochondrial genomes. Curr. Biol. *23*, 553–559.

S3. Rasmussen, M., Guo, X., Wang, Y., Lohmueller, K.E., Rasmussen, S., Albrechtsen, A., Skotte, L., Lindgreen, S., Metspalu, M., Jombart, T., et al. (2011). An Aboriginal Australian genome reveals separate human dispersals into Asia. Science *334*, 94–98.

S4. Meyer, M., Kircher, M., Gansauge, M.-T., Li, H., Racimo, F., Mallick, S., Schraiber, J.G., Jay, F., Prüfer, K., de Filippo, C., et al. (2012). A high-coverage genome sequence from an archaic Denisovan individual. Science *338*, 222–226.

S5. Fu, Q., Li, H., Moorjani, P., Jay, F., Slepchenko, S.M., Bondarev, A.A., Johnson, P.L.F., Aximu-Petri, A., Prüfer, K., de Filippo, C., et al. (2014). Genome sequence of a 45,000-year-old modern human from western Siberia. Nature *514*, 445–449.

S6. Fu, Q., Hajdinjak, M., Moldovan, O.T., Constantin, S., Mallick, S., Skoglund, P., Patterson, N., Rohland, N., Lazaridis, I., Nickel, B., et al. (2015). An early modern human from Romania with a recent Neanderthal ancestor. Nature *524*, 216–219.

S7. Seguin-Orlando, A., Korneliussen, T.S., Sikora, M., Malaspinas, A.-S., Manica, A., Moltke, I., Albrechtsen, A., Ko, A., Margaryan, A., Moiseyev, V., et al. (2014). Paleogenomics. Genomic structure in Europeans dating back at least 36,200 years. Science *346*, 1113–1118.

S8. Raghavan, M., Skoglund, P., Graf, K.E., Metspalu, M., Albrechtsen, A., Moltke, I., Rasmussen, S., Stafford, T.W., Orlando, L., Metspalu, E., et al. (2014). Upper Palaeolithic Siberian genome reveals dual ancestry of Native Americans. Nature *505*, 87–91.

S9. Jones, E.R., Gonzalez-Fortes, G., Connell, S., Siska, V., Eriksson, A., Martiniano, R., McLaughlin, R.L., Gallego Llorente, M., Cassidy, L.M., Gamba, C., et al. (2015). Upper Palaeolithic genomes reveal deep roots of modern Eurasians. Nat. Commun. *6*, 8912.

S10. Lazaridis, I., Patterson, N., Mittnik, A., Renaud, G., Mallick, S., Sudmant, P.H., Schraiber, J.G., Castellano, S., Kirsanow, K., Economou, C., et al. (2014). Ancient human genomes suggest three ancestral populations for present-day Europeans. Nature *513*, 409–413.

S11. Olalde, I., Allentoft, M.E., Sánchez-Quinto, F., Santpere, G., Chiang, C.W.K., DeGiorgio, M., Prado-Martinez, J., Rodríguez, J.A., Rasmussen, S., Quilez, J., et al. (2014). Derived immune and ancestral pigmentation alleles in a 7,000-year-old Mesolithic European. Nature *507*, 225–228.

S12. Mathieson, I., Lazaridis, I., Rohland, N., Mallick, S., Patterson, N., Roodenberg, S.A., Harney, E., Stewardson, K., Fernandes, D., Novak, M., et al. (2015). Genome-wide patterns of selection in 230 ancient Eurasians. Nature *528*, 499–503.

S13. Gamba, C., Jones, E.R., Teasdale, M.D., McLaughlin, R.L., Gonzalez-Fortes, G., Mattiangeli, V., Domboróczki, L., Kővári, I., Pap, I., Anders, A., et al. (2014). Genome flux and stasis in a five millennium transect of European prehistory. Nat. Commun. *5*, 5257.

S14. Skoglund, P., Malmstrom, H., Omrak, A., Raghavan, M., Valdiosera, C., Gunther, T., Hall, P., Tambets, K., Parik, J., Sjogren, K.-G., et al. (2014). Genomic diversity and admixture differs for stone-age Scandinavian foragers and farmers. Science *344*, 747–750.

S15. Hofmanová, Z., Kreutzer, S., Hellenthal, G., Sell, C., Diekmann, Y., Díez-del-Molino, D., van Dorp, L., López, S., Kousathanas, A., Link, V., et al. (2016). Early farmers from across Europe directly descended from Neolithic Aegeans. Proc. Natl. Acad. Sci. *113*, 6886–6891.

S16. Omrak, A., Günther, T., Valdiosera, C., Svensson, E.M., Malmström, H., Kiesewetter, H., Aylward, W., Storå, J., Jakobsson, M., and Götherström, A. (2016). Genomic evidence establishes Anatolia as the source of the European neolithic gene pool. Curr. Biol. *26*, 270–275.

S17. Cassidy, L.M., Martiniano, R., Murphy, E.M., Teasdale, M.D., Mallory, J., Hartwell, B., and Bradley, D.G. (2015). Neolithic and Bronze Age migration to Ireland and establishment of the insular Atlantic genome. Proc. Natl. Acad. Sci. *113*, 201518445.

S18. Keller, A., Graefen, A., Ball, M., Matzas, M., Boisguerin, V., Maixner, F., Leidinger, P., Backes, C., Khairat, R., Forster, M., et al. (2012). New insights into the Tyrolean Iceman's origin and phenotype as inferred by whole-genome sequencing. Nat. Commun. *3*, 698.

S19. Günther, T., Valdiosera, C., Malmström, H., Ureña, I., Rodriguez-Varela, R., Sverrisdóttir, Ó.O., Daskalaki, E.A., Skoglund, P., Naidoo, T., Svensson, E.M., et al. (2015). Ancient genomes link early farmers from Atapuerca in Spain to modern-day Basques. Proc. Natl. Acad. Sci. U. S. A. *112*, 11917–11922.

S20. Haak, W., Lazaridis, I., Patterson, N., Rohland, N., Mallick, S., Llamas, B., Brandt, G., Nordenfelt, S., Harney, E., Stewardson, K., et al. (2015). Massive migration from the steppe was a source for Indo-European languages in Europe. Nature *522*, 207–211.
S21. Allentoft, M.E., Sikora, M., Sjögren, K.-G., Rasmussen, S., Rasmussen, M., Stenderup, J., Damgaard, P.B., Schroeder, H., Ahlström, T., Vinner, L., et al. (2015). Population genomics of Bronze Age Eurasia. Nature *522*, 167–172.
S22. Llorente, M.G., Jones, E.R., Eriksson, A., Siska, V., Arthur, K.W., Arthur, J.W., Curtis, M.C., Stock, J.T., Coltorti, M., Pieruccini, P., et al. (2015). Ancient Ethiopian genome reveals extensive Eurasian admixture in Eastern Africa. Science *350*, 820–822.
S23. Baird, D. (2012). The Late Epipaleolithic, Neolithic, and Chalcolithic of the Anatolian Plateau, 13,000 – 4000 BC. In A Companion To The Archaeology Of The Ancient Near East, D. Potts, ed. (Oxford, UK: Wiley-Blackwell) pp. 431–466.
S24. Baird, D., Asouti, E., Astruc, L., Baysal, A., Baysal, E., Carruthers, D., Fairbairn, A., Kabukcu, C., Jenkins, E., Lorentz, K., et al. (2013). Juniper smoke, skulls and wolves' tails. The Epipalaeolithic of the Anatolian plateau in its South-west Asian context; insights from Pınarbaşı. Levant *45*, 175–209.
S25. Baird, D. Pinarbaşi; from Epipalaeolithic campsite to sedentarising village in central Anatolia. 181–218.
S26. Baird, D., Fairbairn, A., Martin, L., and Middleton, C. (2012). The Boncuklu project: The origins of sedentism, cultivation and herding in central Anatolia. In The Neolithic In Turkey: New Excavations And New Research 3–Central Turkey, M. Özdoğan, N. Başgelen, P. Kuniholm, eds. (Istanbul: Archaeology and Art Publications) pp. 219–244.
S27. Özbaşaran, M., and Duru, G. (2015). The Early Sedentary Community of Cappadocia: Aşıklı Höyük. In La Cappadoce Méridionale De La Préhistoire À La Période Byzantine., D. Beyer, O. Henry, A. Tibet, A. von Haeseler, eds. (İstanbul: IFEA) pp. 43–51.
S28. Stiner, M.C., Buitenhuis, H., Duru, G., Kuhn, S.L., Mentzer, S.M., Munro, N.D., Pöllath, N., Quade, J., Tsartsidou, G., and Özbaşaran, M. (2014). A forager-herder trade-off, from broad-spectrum hunting to sheep management at Aşıklı Höyük, Turkey. Proc. Natl. Acad. Sci. U. S. A. *111*, 8404–8409.
S29. Esin, U. (1996). Aşıklı, ten thousand years ago: a habitation model from Central Anatolia. In Housing And Settlement In Anatolia: A Historical Perspective, (İstanbul: Tarih Vakfı Yayınları) pp. 31–42.
S30. French, D. (1972). Excavations at Can Hasan lll, 1969- 1970. In Papers In Economic Prehistory, (Cambridge: University Press) pp. 182–188.
S31. Balkan-Atlı, N. and Binder, D. (2012). Neolithic obsidian workshop at Kömürcü-Kaletepe (Central Anatolia). In The Neolithic In Turkey. New Excavations And New Research 3 - Central Turkey, M. Ozdoğan, N. Başgelen, P. Kuniholm, eds. (İstanbul: Archaeology and Art Publications) pp. 71–88.
S32. Binder, D. (2001). Stones making sense: What obsidian could tell about the origins of the central Anatolian Neolithic Proc Interational CaneW Table Ronde (Istanbul: Ege Publishing Co.) pp. 79–90.
S33. Bıçakçı, E., Godon, M., and Çakan, Y.G. (2012). Tepecik-Çiftlik. In Neolithic In Turkey: New Excavations And New Research 3–Central Turkey, M. Ozdoğan, N. Başgelen, P. Kuniholm, eds. (İstanbul: Archaeology and Art Publications) pp. 89–134.
S34. Hodder, I. (2012). Çatal Höyük. In Neolithic In Turkey: New Excavations And New Research 3-Central Turkey, M. Ozdoğan, N. Başgelen, P. Kuniholm, eds. (İstanbul: Archaeology and Art Publications) pp. 245–277.
S35. Mellaart, J. (1967). Çatal Hüyük. A Neolithic Town In Anatolia, (New York: McGraw-Hill).
S36. Büyükkarakaya, A.M., Erdal, Y.S. (2014). New Data on Mortuary Practices from the Early Pottery Neolithic Site of Tepecik-Çiftlik, Central Anatolia 20th Annu Meet Eur Assoc Archaeol (İstanbul:) pp. 525.
S37. Ottoni, C., Ricaut, F.-X., Vanderheyden, N., Brucato, N., Waelkens, M., and Decorte, R. (2011). Mitochondrial analysis of a Byzantine population reveals the differential impact of multiple historical events in South Anatolia. Eur. J. Hum. Genet. *19*, 571–576.
S38. Dabney, J., Knapp, M., Glocke, I., Gansauge, M.-T., Weihmann, A., Nickel, B., Valdiosera, C., García, N., Pääbo, S., Arsuaga, J.-L., et al. (2013). Complete mitochondrial genome sequence of a Middle Pleistocene cave bear reconstructed from ultrashort DNA fragments. Proc. Natl. Acad. Sci. U. S. A. *110*, 15758–15763.
S39. Meyer, M., and Kircher, M. (2010). Illumina sequencing library preparation for highly multiplexed target capture and sequencing. Cold Spring Harb. Protoc. *5*, prot5448.
S40. Kircher, M. (2012). Analysis of high-throughput ancient DNA sequencing data. In Ancient DNA, B. Shapiro, M. Hofreiter, eds. (New York: Humana Press) pp. 197–228.
S41. Li, H., and Durbin, R. (2009). Fast and accurate short read alignment with Burrows-Wheeler transform. Bioinformatics *25*, 1754–1760.
S42. Hofreiter, M., Jaenicke, V., Serre, D., von Haeseler, A., and Pääbo, S. (2001). DNA sequences from multiple amplifications reveal artifacts induced by cytosine deamination in ancient DNA. Nucleic Acids

Res. *29*, 4793–4799.
S43. Hansen, A., Willerslev, E., Wiuf, C., Mourier, T., and Arctander, P. (2001). Statistical evidence for miscoding lesions in ancient DNA templates. Mol. Biol. Evol. *18*, 262–265.
S44. Skoglund, P., Northoff, B.H., Shunkov, M. V, Derevianko, A.P., Pääbo, S., Krause, J., and Jakobsson, M. (2014). Separating endogenous ancient DNA from modern day contamination in a Siberian Neandertal. Proc. Natl. Acad. Sci. U. S. A. *111*, 2229–2234.
S45. Li, H., Handsaker, B., Wysoker, A., Fennell, T., Ruan, J., Homer, N., Marth, G., Abecasis, G., and Durbin, R. (2009). The sequence alignment/map format and SAMtools. Bioinformatics *25*, 2078–2079.
S46. Rasmussen, M., Guo, X., Wang, Y., Lohmueller, K.E., Rasmussen, S., Albrechtsen, A., Skotte, L., Lindgreen, S., Metspalu, M., Jombart, T., et al. (2011). An Aboriginal Australian genome reveals separate human dispersals into Asia. Science *334*, 94–98.
S47. Behar, D.M., Van Oven, M., Rosset, S., Metspalu, M., Loogvali, E.L., Silva, N.M., Kivisild, T., Torroni, A., and Villems, R. (2012). A "copernican" reassessment of the human mitochondrial DNA tree from its root. Am. J. Hum. Genet. *90*, 675–684.
S48. Vianello, D., Sevini, F., Castellani, G., Lomartire, L., Capri, M., and Franceschi, C. (2013). HAPLOFIND: A new method for high-throughput mtDNA haplogroup assignment. Hum. Mutat. *34*, 1189–1194.
S49. van Oven, M., and Kayser, M. (2009). Updated comprehensive phylogenetic tree of global human mitochondrial DNA variation. Hum. Mutat. *30*, E386–E394.
S50. Brandt, G., Haak, W., Adler, C.J., Roth, C., Szecsenyi-Nagy, A., Karimnia, S., Moller-Rieker, S., Meller, H., Ganslmeier, R., Friederich, S., et al. (2013). Ancient DNA reveals key stages in the formation of central European mitochondrial genetic diversity. Science *342*, 257–261.
S51. Briggs, A.W., Stenzel, U., Johnson, P.L.F., Green, R.E., Kelso, J., Prüfer, K., Meyer, M., Krause, J., Ronan, M.T., Lachmann, M., et al. (2007). Patterns of damage in genomic DNA sequences from a Neandertal. Proc. Natl. Acad. Sci. U. S. A. *104*, 14616–14621.
S52. Szécsényi-Nagy, A., Brandt, G., Haak, W., Keerl, V., Möller-Rieker, S., Köhler, K., Mende, B.G., Oross, K., Marton, T., Osztás, A., et al. (2015). Tracing the genetic origin of Europe's first farmers reveals insights into their social organization. Philos. Trans. R. Soc. B Biol. Sci. *282*, 20150339.
S53. Fernández, E., Pérez-Pérez, A., Gamba, C., Prats, E., Cuesta, P., Anfruns, J., Molist, M., Arroyo-Pardo, E., and Turbón, D. (2014). Ancient DNA analysis of 8000 B.C. Near Eastern farmers supports an early neolithic pioneer maritime colonization of Mainland Europe through Cyprus and the Aegean Islands. PLoS Genet. *10*, e1004401.
S54. Derenko, M., Malyarchuk, B., Grzybowski, T., Denisova, G., Dambueva, I., Perkova, M., Dorzhu, C., Luzina, F., Lee, H.K., Vanecek, T., et al. (2007). Phylogeographic analysis of mitochondrial DNA in northern Asian populations. Am. J. Hum. Genet. *81*, 1025–1041.
S55. Bramanti, B., Thomas, M.G., Haak, W., Unterlaender, M., Jores, P., Tambets, K., Antanaitis-Jacobs, I., Haidle, M.N., Jankauskas, R., Kind, C.-J., et al. (2009). Genetic discontinuity between local hunter-gatherers and central Europe's first farmers. Science *326*, 137–140.
S56. Richards, M., Macaulay, V., Hickey, E., Vega, E., Sykes, B., Guida, V., Rengo, C., Sellitto, D., Cruciani, F., Kivisild, T., et al. (2000). Tracing European founder lineages in the Near Eastern mtDNA pool. Am. J. Hum. Genet. *67*, 1251–1276.
S57. Skoglund, P., Malmstrom, H., Raghavan, M., Stora, J., Hall, P., Willerslev, E., Gilbert, M.T.P., Gotherstrom, A., and Jakobsson, M. (2012). Origins and genetic legacy of Neolithic farmers and hunter-gatherers in Europe. Science *336*, 466–469.
S58. Skoglund, P., Storå, J., Götherström, A., and Jakobsson, M. (2013). Accurate sex identification of ancient human remains using DNA shotgun sequencing. J. Archaeol. Sci. *40*, 4477–4482.
S59. Patterson, N., Moorjani, P., Luo, Y., Mallick, S., Rohland, N., Zhan, Y., Genschoreck, T., Webster, T., and Reich, D. (2012). Ancient admixture in human history. Genetics *192*, 1065–1093.
S60. McVean, G.A., Altshuler (Co-Chair), D.M., Durbin (Co-Chair), R.M., Abecasis, G.R., Bentley, D.R., Chakravarti, A., Clark, A.G., Donnelly, P., Eichler, E.E., Flicek, P., et al. (2012). An integrated map of genetic variation from 1,092 human genomes. Nature *491*, 56–65.
S61. Danecek, P., Auton, A., Abecasis, G., Albers, C. a, Banks, E., DePristo, M. a, Handsaker, R.E., Lunter, G., Marth, G.T., Sherry, S.T., et al. (2011). The variant call format and VCF tools. Bioinformatics *27*, 2156–2158.
S62. Patterson, N., Price, A.L., and Reich, D. (2006). Population structure and eigen analysis. PLoS Genet. *2*, e190.
S63. Alexander, D.H., Novembre, J., and Lange, K. (2009). Fast model-based estimation of ancestry in unrelated individuals. Genome Res. *19*, 1655–1664.
S64. Purcell, S., Neale, B., Todd-Brown, K., Thomas, L., Ferreira, M.A.R., Bender, D., Maller, J., Sklar, P., de Bakker, P.I.W., Daly, M.J., et al. (2007). PLINK: A tool set for whole-genome association and

population-based linkage analyses. Am. J. Hum. Genet. *81*, 559–575.

S65. Sikora, M., Carpenter, M.L., Moreno-Estrada, A., Henn, B.M., Underhill, P.A., Sánchez-Quinto, F., Zara, I., Pitzalis, M., Sidore, C., Busonero, F., et al. (2014). Population genomic analysis of ancient and modern genomes yields new insights into the genetic ancestry of the Tyrolean Iceman and the genetic structure of Europe. PLoS Genet. *10*, e1004353.

S66. Jakobsson, M., and Rosenberg, N.A. (2007). CLUMPP: A cluster matching and permutation program for dealing with label switching and multimodality in analysis of population structure. Bioinformatics *23*, 1801–1806.

S67. Pickrell, J.K., and Pritchard, J.K. (2012). Inference of population splits and mixtures from genome-wide allele frequency data. PLoS Genet. *8*, e1002967.